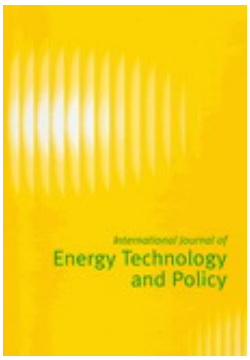

International Journal of Energy Technology and Policy

ISSN online: 1741-508X - ISSN print: 1472-8923
https://www.inderscience.com/ijetp

Low voltage current transformer defect detection method based on Hausdorff distance algorithm under charged state

Kai Sun, Xiaohui Zhai, Yanling Sun, Yan Du, Yuning Fa

DOI: 10.1504/IJETP.2024.10061518

Article History:

Received:	21 June 2023
Last revised:	04 August 2023
Accepted:	19 October 2023
Published online:	10 May 2024

Low voltage current transformer defect detection method based on Hausdorff distance algorithm under charged state

Kai Sun*, Xiaohui Zhai, Yanling Sun, Yan Du and Yuning Fa

Marketing Service Center (Metering Center),
State Grid Shandong Electric Power Company,
Jinan, 250000, China
Email: 15662799686@163.com
Email: dkyzxh@163.com
Email: 6913syl@163.com
Email: Duyan1206@163.com
Email: ayuning1532@163.com
*Corresponding author

Abstract: In order to accurately detect the defects of low-voltage current transformers, a defect detection method of low-voltage current transformers based on Hausdorff distance algorithm under charged state is proposed. In the charged state, the noise variance of the defect image of low-voltage current transformer is calculated, the grey variance in the bilateral filter function is adjusted, and the defect image of low-voltage current transformer after noise removal is obtained. The Canny edge results are calculated to obtain the distance transform map. The mask convolution processing is performed on the distance transform map to cluster the results, and then the defect characteristics of different types of low-voltage current transformers are obtained. At the same time, the Hausdorff distance algorithm and elastic graph matching are effectively combined to realise defect detection of low-voltage current transformers. The experimental results show that the proposed method can quickly and accurately detect the defects of low-voltage current transformers.

Keywords: charged state; Hausdorff distance algorithm; low voltage current transformer; defect detection.

Reference to this paper should be made as follows: Sun, K., Zhai, X., Sun, Y., Du, Y. and Fa, Y. (2024) 'Low voltage current transformer defect detection method based on Hausdorff distance algorithm under charged state', *Int. J. Energy Technology and Policy*, Vol. 19, Nos. 1/2, pp.65–85.

Biographical notes: Kai Sun graduated from Shandong University with a Master of Engineering degree in Electronics and Communication Engineering. He is currently engaged in electrical energy measurement related work, with research topics including acquisition equipment detection technology, transformer calibration technology, fibre optic communication, image processing, etc.

Xiaohui Zhai is a Senior Engineer. Her main research direction is engaged in the research of electric energy measurement technology, automatic verification and detection technology of electricity meters and transformers, key technology of integrated current and voltage sensing and measurement technology of transformer value transfer.

Yanling Sun is a Senior Engineer with a Bachelor's degree in Electrical Engineering and Automation from Shandong University of Technology. Currently, she is engaged in research on power measurement and testing technology, with rich experience in the verification and testing of energy meters, transformers, and acquisition terminals.

Yan Du obtained her Master's degree in Power System and Automation from Huazhong University of Science and Technology in 2012. Currently, she is a Senior Engineer at State Grid Shandong Marketing Service Center. She has a rich research experience in DC energy metering technology, electricity information collection, electricity load perception, and high-level standard electricity metering.

Yuning Fa graduated from Qingdao University of Technology with a major in Electrical Engineering and Automation. He has been engaged in electrical energy measurement for a long time and has a rich experience in the measurement and detection technology of power transformers for measurement.

1 Introduction

Low voltage current transformer plays an important role in power system, which is used for current measurement and protection applications. However, due to long-term use, environmental factors and inevitable problems during manufacturing and installation, low-voltage current transformers may have various defects, such as internal short circuit, insulation breakdown, coil fault, etc. These defects can lead to a decrease in transformer performance, and even bring safety hazards and power grid accidents. By developing effective defect detection methods, real-time monitoring and fault warning of low-voltage current transformers can be realised. This helps to detect the abnormal state of the transformer in advance and take corresponding maintenance or replacement measures to avoid potential equipment failures and production interruptions. The research on defect detection methods can also improve the reliability and stability of power systems. Low voltage current transformer is the key sensor equipment in power system, which plays a vital role in power grid monitoring and protection. By accurately detecting the defects of the transformer, timely measures can be taken to repair or replace damaged transformers, improving the reliability and stability of the power system. The research on the defect detection method of low-voltage current transformer is also helpful to promote the development and improvement of power equipment technology. By deeply understanding the defect types, formation mechanisms, and detection methods of transformers, valuable reference and guidance can be provided for the design and manufacturing of transformers, continuously improving the quality and performance of transformers. Therefore, the research on defect detection methods of low-voltage current transformers has important practical and theoretical significance, and has a positive role in promoting the safety, reliability and economy of power systems (Guo et al., 2022; Yu et al., 2023).

Relevant domestic experts have carried out a lot of research on the defect detection of low-voltage current transformers. Hu et al. (2021) give priority to a small number of normal texture sample images as training sets, mainly for the training of network models; By artificially setting missing areas in the sample image, a network model is used to

predict the content of the missing parts; Finally, defect detection is achieved by evaluating the structural similarity and residual between the reconstructed image and the image to be tested. Luo and Xu (2021) prioritise image unfolding and filtering processing; Then, the key features of the defect image are enhanced through HSV spatial transformation; Finally, the improved faster R-CNN convolutional neural network is introduced to complete the image surface defect detection. Wang et al. (2021a) mainly used an improved CenterNet network for defect detection on image surfaces. Although the above method can complete the defect detection of low-voltage current transformer, it has the problems of high miss detection rate, high false detection rate and long detection time.

Aiming at the problems of the above methods, a defect detection method of low-voltage current transformer based on Hausdorff distance algorithm under live state is proposed. The detailed research plan for this method is as follows:

1 in order to improve the reliability of defect detection of low-voltage current transformer, a bilateral filtering method is used to denoise the defect image of low-voltage current transformer

2 based on the denoised defect image of low-voltage current transformer, Canny algorithm is used to extract the features of defect image

3 the elastic graph matching algorithm and Hausdorff distance algorithm are effectively combined to detect the defects of low-voltage current transformer in the electrified state and obtain the final defect detection results.

2 Defect detection of low-voltage current transformer under electrification

2.1 Image denoising processing of transformer defects

In order to improve the detection accuracy of transformer defects, it is first necessary to denoise the transformer defect image.

The emergence of bilateral filtering algorithm (Hasan et al., 2021; Kong et al., 2021) effectively overcomes the shortcomings of traditional image denoising methods. It can effectively expand the nonlinear combination of grey information and spatial information of the defect image of low-voltage current transformer, and is mainly used for the denoising of the defect image of low voltage current transformer (Wang et al., 2021b; Riya et al., 2021).

Set Z to represent the defect image of low-voltage current transformer in the electrified state after noise removal, and p to be a random pixel in Z. If the known pixel value is U_p, the bilateral filtering model can be expressed in the following form:

$$Z(p) = \frac{\sum_{p\in 1} L_p I_p U_p}{\sigma} \tag{1}$$

In the above equation, $Z(p)$ represents the bilateral filtering model; L_p represents the weight coefficient of the space domain; I_p represents the weight coefficient of the grayscale domain; σ represents a normalised constant, and the corresponding expression is as follows:

$$\sigma = \sum\nolimits_{p\in 1} L_p I_p \tag{2}$$

L_p and I_p are expressed in the form of formulas (3) and (4), respectively:

$$L_p = \exp\left[\frac{\|p-q\|^2}{2\omega_k^2}\right] \tag{3}$$

$$I_p = \exp\left[\frac{\|f_p - f_q\|^2}{2\omega_h^2}\right] \tag{4}$$

In the above formula, ω_k and ω_h represent spatial and grey variance; q stands for space domain; f represents the defect image of low-voltage current transformer, which can be expressed in the form of formula (5):

$$f = Z + n \tag{5}$$

In the above equation, n represents additive noise.

It can be seen from formula (3) that the spatial domain weight coefficient L_p is a Gaussian function related to spatial variance ω_k; As the value of ω_k increases, the value of L_p also increases, resulting in a smoother Gaussian curve and significant smoothing effect. However, the overall image becomes blurry; on the contrary, the value of L_p will decrease, and the clarity of the image will be improved to some extent, but some noise still exists in the image. Since most of the Gaussian function is concentrated in $[-2\omega_k, 2\omega_k]$, ω_k can be obtained by the following formula:

$$\omega_k = \frac{r}{2} \tag{6}$$

In the above equation, r represents the radius value corresponding to the bilateral filtering template.

The grey variance ω_h has a greater impact on bilateral filtering denoising. When the value of ω_h is relatively large, it indicates that the noise in the defect image of low-voltage current transformer under electrification can be effectively filtered, but the image will be blurred. Among them, ω_h and noise variance ω_a belong to a linear relationship, and the proportion between the two is between. In order to ensure that the detail information of the defect image of the low-voltage current transformer is effectively preserved after the denoising process (Qu et al., 2021; Guo et al., 2021), ω_h needs to be obtained, but ω_a needs to be obtained first. To this end, adjust the greyscale variance according to actual needs, effectively filtering out noise in the image.

Set b_1, b_2, …, b_n to represent the n observation data obtained in a constant state, and use the probability distribution function $h(b_i)$ to describe the observation data using noise variance. The corresponding calculation formula is as follows:

$$h(b_i) = \prod\nolimits_{i=1}^{n} \frac{b_i}{\omega_a} e^{\frac{\omega_a}{2\omega_a+1}} Z_0\left(\frac{2\omega_k^2}{2\omega_h^2}\right) \tag{7}$$

In the above equation, Z_0 represents the modified Bessel function.

The corresponding signal strength $InX(A)$ can be obtained through the maximum Likelihood function, as shown in formula (8):

$$InX(A)=\sum_{i=1}^{n} In\left(\frac{Ab_n}{\omega_a}\right)-\sum_{i=1}^{n}\left(\frac{Ab_n+1}{\omega_a}\right)+\sum_{i=1}^{n} Z_0\left(\frac{Ab_n+1}{\omega_a}\right) \tag{8}$$

By obtaining the global maximum value of $InX(A)$, ω_a can be obtained, and the corresponding calculation formula is as follows:

$$\omega_a^2=\arg\max\{InX(A)\} \tag{9}$$

In the process of bilateral filtering, L_p can restrict I_p, resulting in a large difference between the edge and other details of the low-voltage current transformer defect image in the charged state and the central pixel, and the corresponding spatial domain coefficient weight coefficient will also be reduced, thus ensuring that more information in the image can be effectively retained. However, strong noise also meets the requirement of having a relatively large difference from the central pixel, so it is effectively preserved in bilateral filtering. After ω_a is obtained through formula (9), the double side filtering algorithm can be used to denoise the defect image of low-voltage current transformer in the charged state (Wan et al., 2021; Fan et al., 2021), and obtain the denoised image $f(x, y)$ as shown in formula (10):

$$f(x,y)=\frac{\sum_{i=1}^{n} In\left(\frac{Ab_n}{\omega_a}\right)}{\omega_a^2\left(L_p-I_p\right)} \tag{10}$$

2.2 Defect feature extraction of low-voltage current transformer

After the denoising of the defect image of the transformer, in order to describe the defect of the transformer more effectively, it is necessary to extract the defect features of the low-voltage current transformer.

In the electrified state, the edge of the low-voltage current transformer image refers to the part of the area where the brightness changes significantly, which can be regarded as a step, that is, the area with a small grey value is quickly transformed into a buffer area with a large grey value. In the process of using the Canny algorithm, the following three principles should be paid attention to:

1 it has a relatively good signal-to-noise ratio, which means that non-edge points should not be detected, and edge points should not have false or missed detections

2 having a unique response to a single edge while minimising the response to false edges

3 it has good positioning function, which ensures the shortest distance between the detected edge point and the actual edge.

The detailed operation steps of the Canny algorithm are shown in Figure 1.

Figure 1 Canny algorithm operation flow chart

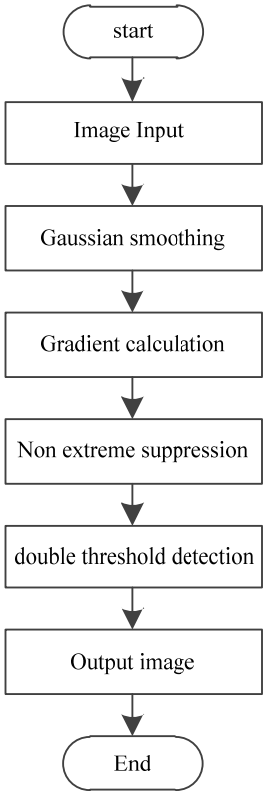

Set the filter function of edge detection as $I(x)$. In the case of the noise type in the defect image of the low-voltage current transformer under the electrified state, combined with the corresponding criteria of edge detection, the corresponding formulas of signal to noise ratio SNR, positioning accuracy M and average proximity N of the false boundary can be obtained as follows:

$$\begin{cases} SNR = \dfrac{\left|\int_{-\infty}^{0} I(x)dx\right|}{\left[\beta\sqrt{\int_{-\infty}^{+\infty} I(x)dx}\right]} \\ M = \dfrac{I(x)}{\left[\beta\sqrt{\int_{-\infty}^{+\infty} I(x)dx}\right]} \\ N = \sqrt{\dfrac{\int_{-\infty}^{+\infty} I(x)dx}{\beta\sqrt{\int_{-\infty}^{+\infty} I(x)dx}}} \end{cases} \tag{11}$$

In the above equation, β represents the noise variance.

In the process of using the Canny algorithm, the optimal product of signal-to-noise ratio and positioning accuracy is obtained in a limited area, and the Canny operator $Cn(x)$ is given by formula (12):

$$Cn(x) = xe^{-\frac{ax}{2}} \tag{12}$$

In the above formula, $xe^{-\frac{ax}{2}}$ represents Gaussian function; x represents a constant.

DT transform is a special Binary image transform method. The image obtained after DT transform processing is a greyscale image, also known as a distance image. Provide a schematic diagram of DT transformation through Figure 2.

Figure 2 Schematic diagram of DT transformation

0	0	0	0	0
0	0	0	0	0
0	0	1	0	0
0	0	0	0	0
0	0	0	0	0

(a)

2.8	2.2	2.0	2.2	2.8
2.2	1.4	1.0	1.4	2.2
2.0	1.0	0	1.0	2.0
2.2	1.4	1.0	1.4	2.2
2.8	2.2	2.0	2.2	2.8

(b)

In combination with the above analysis, Canny algorithm and DT transform are effectively combined to carry out feature extraction operation (Hwang et al., 2022; Wei and Zhang, 2021) on the defect image of low-voltage current transformer under charged state. The detailed operation steps are as follows:

1 Read in the defect feature image $f(x, y)$ of low-voltage current transformer under electrification.

2 Canny edge extraction is carried out for the defect feature image $f(x, y)$ of low-voltage current transformer under electrification, and it is represented as $D(x, y)$.

3 The corresponding calculation formula for the DT transformation operation $DT(x, y)$ of image $D(x, y)$ is as follows:

$$DT(x, y) = \min\left(sqrt(x' - x) + (y' - y)^2\right), (x', y') \in D(x, y), D(x', y') = 1 \tag{13}$$

4 The binary segmentation processing is carried out for $DT(x, y)$ to effectively filter out the small detail texture in the defect image of low-voltage current transformer under the charged state, and the obtained result is expressed as $BW(x, y)$.

5 The mask convolution operation is carried out for $BW(x, y)$ to effectively filter the false edges in the defect image of low-voltage current transformer under the charged state. The corresponding calculation formula is as follows:

$$Rslt = \sum_{i=v}^{u+m} \sum_{j=t}^{u+m} BW(i, j) * Msk(i, j) \tag{14}$$

In the above equation, *Msk* represents that except for the image boundary value of 1, all remaining mask values are 0; u and t represent the horizontal and vertical coordinates of the mask; m represents a constant.

6 The image after the mask convolution is processed by Euclidean distance expansion clustering, the cluster centre is calculated by hierarchical clustering method, and the rectangular feature vertex is calculated by geometric constraint relationship, so as to obtain the defect characteristics of low-voltage current transformer in the charged state (Yang et al., 2021a).

2.3 Low voltage current transformer defect detection based on Hausdorff distance algorithm

Hausdorff distance is a distance measurement method that measures the similarity or difference between two point sets. It is based on the maximum distance between pairs of points that are closest to each other between point sets. When it comes to defect detection of low-voltage current transformers, Hausdorff distance algorithm has several advantages. Firstly, it keenly captures small differences and shape changes in point sets, effectively distinguishing the size and shape of defects. Secondly, it is not affected by the order of point set arrangement and maintains good flexibility and robustness. In addition, the results are easy to understand, intuitive and interpretable, and can directly display the maximum difference between two point sets. Finally, this algorithm is applicable to transformers of different sizes and shapes, and can also be applied to some point cloud data. In conclusion, Hausdorff distance algorithm provides accurate and reliable results in defect detection of low-voltage current transformers, which is of great significance for enhancing the security and stability of power system.

Hausdorff distance algorithm is a basic concept in distance pattern recognition, which can be divided into the following types:

1 geometric measurement

2 similarity measurement.

Hausdorff distance is mainly used to define the maximum and minimum distances between two random point sets, which measure the degree of matching between two

point sets. Given two finite point sets $A = \{a_1, a_2, \ldots, a_n\}$ and $B = \{b_1, b_2, \ldots, b_n\}$ first, the Hausdorff distance $D(A, B)$ between the two point sets A and B can be expressed in the form of formula (15):

$$D(A, B) = \max\{d(A, B), d(B, A)\} \tag{15}$$

In the above equation, $d(A, B)$ and $d(B, A)$ represent the finite Hausdorff distances from point set A to B and from point set B to A. The corresponding calculation formulas for the two are as follows:

$$\begin{cases} d(A, B) = \max\limits_{a \in A} \min\limits_{b \in B} \|a - b\| \\ d(A, B) = \max\limits_{b \in B} \min\limits_{a \in A} \|b - a\| \end{cases} \tag{16}$$

The Hausdorff distance can accurately describe the pixel lines between different Binary image. Among them, the Hausdorff distance algorithm mainly has the following properties:

1 when point set A to point set B are all closed sets, the three axioms set need to be satisfied.

2 normally, $d(A, B) \neq d(B, A)$.

Elastic graph matching algorithm is a very important recognition method, which has been widely applied in the field of image recognition (Yang et al., 2021b; Yao et al., 2021). In the practical application process, the defect detection of low-voltage current transformer can be regarded as the matching process between the establishment of template elasticity diagram and the defect image of low-voltage current transformer to be tested. The defect template of low-voltage current transformer in the template library stores the key feature points and location information of the defect area of low-voltage current transformer, which can accurately reflect the defect status of low-voltage current transformer. Therefore, the matching is carried out using an elastic template matching algorithm based on the minimum energy function, and the energy function $F(m)$ is expressed in the form of formula (17):

$$F(m) = \sum\nolimits_{i=1} -ci \left| \frac{(c_i, y_j)}{\|c_i\| y_j \|\|} \right| + \alpha \sqrt{\Delta e_x^2 + \Delta e_y^2} \tag{17}$$

In the above formula, c_i represents the defect characteristic vector of low-voltage current transformer under the i electrified state in the template; y_i represents the defect characteristic vector of low-voltage current transformer under the j electrified state in the template; α represents the influence factor corresponding to the energy function; Δe_x^2 and Δe_y^2 represent the deformation variables of defect characteristics of low-voltage current transformer in x direction and y direction under the i electrification state.

At this stage, more and more people apply template matching method to defect detection of low-voltage current transformer, which occupies a very important position in the field of pattern recognition. It can obtain satisfactory robustness in the light and attitude interference environment. The elastic template matching algorithm is to perform elastic matching between the key feature vectors extracted from the template image and the feature vectors of the image to be detected. The main implementation process is to

correspond the defect feature vectors in the template image to the image to be tested, and during the similarity calculation process, each pixel point in the key defect area of the template moves within a pixel unit to obtain the minimum similarity between the two defect features. Among them, the Euclidean distance in the n dimensional space is expressed in the form of formula (18):

$$l = \sqrt{\sum (x_{i1} - x_{i2})^2} \tag{18}$$

In the above equation, x_{i1} and x_{i2} represent the dimensionality coordinates corresponding to the first and second points in the set dimension space.

The similarity $L_{x,y}$ is given by formula (19):

$$\begin{cases} L_{x,y} = \min(L(T(x-1, y))J(x, y), L(T(x, y)J(x, y)), L(T(x+1, y)), \\ \qquad J(x, y), L(T(x, y-1), y), J(x, y)) \\ L(T, I) = \sum_x \sum_y L_{x,y} \end{cases} \tag{19}$$

(19)

In the above formula, x and y represent the coordinate position of each pixel in the defect image of low-voltage current transformer under the charged state; T and I represent the feature vector extracted from the key features in the defect image of low-voltage current transformer under the charged state and the feature vector of the image to be detected; $L(T, I)$ represents the elastic movement distance.

On the basis of the above analysis, it is necessary to effectively combine the elastic diagram matching algorithm and the Hausdorff distance algorithm to detect the defects of the low-voltage current transformer under the charged state. The detailed operation steps are as follows:

1 Template initialisation processing:

   First, CEGragh is used to store the elastic map of the defect image of low-voltage current transformer in the electrified state, and then the defect features in the template are extracted and stored in CEGragh.

2 Select the defect image of low-voltage current transformer under the state of waiting for electrification to be detected, and store the extracted features in CEGragh.

3 Set offset:

   The template can expand the small overall deviation of the defect image of low-voltage current transformer under the charged state to be detected, and the minimum value selected will be taken as the final result.

4 Calculate the similarity between two images using the Hausdorff distance algorithm:
   a set the weight value of the key defect area and key area of the low-voltage current transformer under the charged state
   b expand the elastic graph matching operation through the minimum energy function
   c obtain the maximum degree of mismatch using the Hausdorff distance algorithm and save it.

5 Repeat steps 3 and 4 to obtain all Hausdorff distances, so as to describe the maximum mismatch between the low-voltage current transformer image to be detected in the charged state and the low-voltage current transformer defect characteristics in the charged state, and realise the low-voltage current transformer defect detection in the charged state.

3 Experimental analysis

3.1 Experimental data

In the experiment, defect images of some low-voltage current transformers with noise under charged state are selected as test samples for experimental analysis, as shown in Figure 3.

Figure 3 Partial test sample images (see online version for colours)

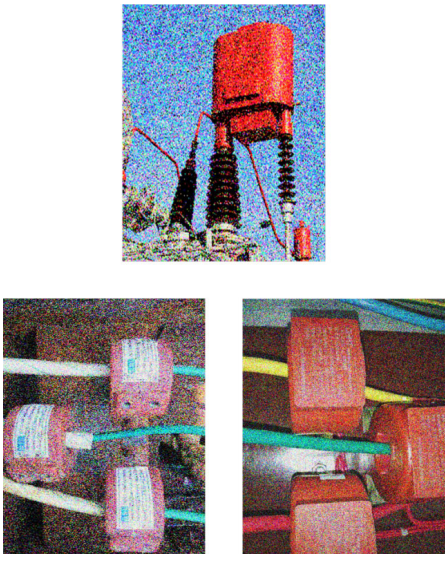

3.2 Experimental plan and indicators

In order to effectively verify the superiority and effectiveness of the proposed method, wavelet transform and median filtering were mainly selected as comparative methods in the denoising experiment; in the detection experiment, method of Hu et al. (2021), method of Luo and Xu (2021), and method of Wang et al. (2021a) were selected as comparative methods.

The experiment mainly carries out experimental analysis from three aspects of noise removal performance, that is, signal-to-noise ratio, root-mean-square deviation and noise removal time consumption. At the same time, it also needs to verify the defect detection performance of low-voltage current transformer, mainly from three aspects of false detection rate, missing detection rate and detection time.

3.3 Experimental results

The experiment gives priority to de-noising the defect image of low-voltage current transformer by various methods, and the experimental results obtained are shown in Figure 4.

Figure 4 Comparison of denoising results of defect images of low-voltage current transformers by different methods, (a) proposed method (b) wavelet transform method (c) median filtering method (see online version for colours)

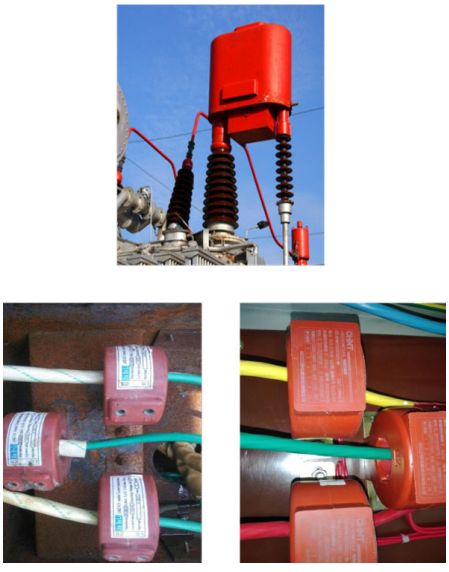

(a)

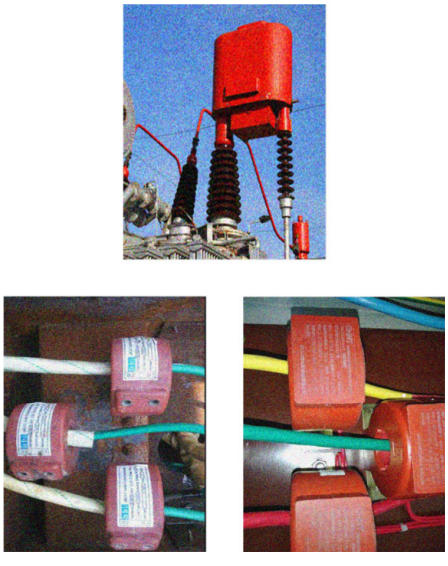

(b)

Figure 4 Comparison of denoising results of defect images of low-voltage current transformers by different methods, (a) proposed method (b) wavelet transform method (c) median filtering method (continued) (see online version for colours)

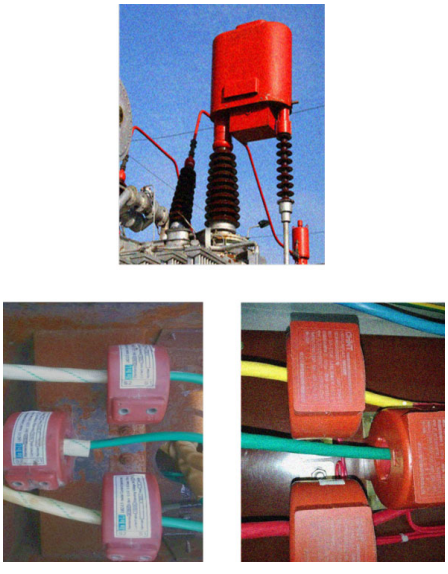

(c)

It can be seen from the analysis of Figure 4 that the proposed method can effectively filter the noise in the image after denoising the defect image of low-voltage current transformer containing noise, and the overall denoising effect is relatively ideal; after the wavelet transform method and median filtering method are used to denoise the defect image of low-voltage current transformer, although most of the noise in the image can be effectively filtered, there is still some noise pollution, and the overall denoising effect is poor.

The formula corresponding to root-mean-square deviation *RMSE* is given by formula (20):

$$RMSE = \sqrt{\frac{\sum_{i=1}^{n}\sum_{j=1}^{n}\left[Z_p(i,\,j) - Z(i,\,j)\right]^2}{m \times n}} \tag{20}$$

In the above formula, $Z_p(i,\,j)$ represents the defect image of low-voltage current transformer after noise elimination; $z(i,\,j)$ represents the defect image of low-voltage current transformer without noise. The calculation formula for signal-to-noise ratio is given using formula (11). The larger the value of *SNR*, the better the noise smoothing effect; The smaller the value of *RMSE*, the closer the denoised image is to the noiseless image, indicating a better denoising effect.

The comparison of experimental results of signal to noise ratio and Root-mean-square deviation corresponding to each denoising method is given in Tables 1 and 2.

Table 1 Comparison of signal-to-noise ratio experimental results of different denoising methods

Test image number	*Signal to noise ratio (dB)*		
	Proposed method	*Wavelet transform method*	*Wavelet transform method*
01	3.54	3.33	3.14
02	4.01	3.87	3.60
03	3.63	3.52	3.44
04	3.88	3.64	3.52
05	4.17	4.08	4.01
06	4.55	4.32	4.26
07	3.99	3.84	3.79
08	4.06	3.96	3.90
09	3.03	2.73	2.66
10	3.52	3.41	3.26

Table 2 Comparison of root-mean-square deviation experimental results of different denoising methods

Test image number	*root mean square error*		
	Proposed method	*Wavelet transform method*	*Wavelet transform method*
01	8.75	9.52	9.88
02	6.54	7.16	7.57
03	2.50	3.56	3.76
04	3.69	4.22	4.50
05	7.41	7.84	7.95
06	4.55	5.12	5.43
07	6.02	6.30	6.45
08	5.78	6.01	6.14
09	4.66	5.00	5.08
10	4.74	5.11	5.26

Through the analysis of experimental data in Tables 1 and 2, it can be seen that the proposed method can achieve relatively ideal denoising effects, while the signal-to-noise ratio and mean square error obtained by the other two denoising methods are significantly poor, indicating that the two denoising methods still need further improvement. This is because the proposed method uses bilateral filtering as the denoising method, and its good denoising effect has the following reasons: First, Bilateral filter can remove high-frequency noise, and effectively eliminate noise from measurement error or environmental interference by considering the similarity of spatial position and pixel value at the same time. Secondly, the bilateral filter performs well in preserving edge information, does not blur edges and details, and is conducive to maintaining important edge features. Finally, by properly adjusting the filter parameters, the bilateral filter can balance the filtering effect, remove noise and retain useful details.

Three different methods are given in Figure 5 to carry out experimental comparison on the time spent in image denoising of low-voltage current transformer defects.

Figure 5 Comparison of experimental results of denoising time of defect image of low-voltage current transformer with different denoising methods, (a) proposed method (b) wavelet transform method (c) weighted median filter (see online version for colours)

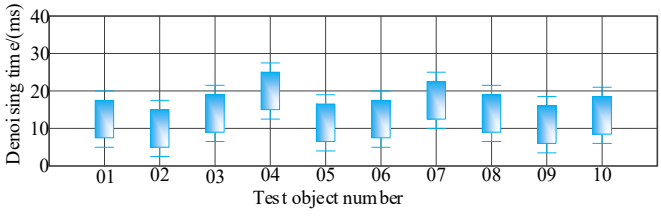

(a)

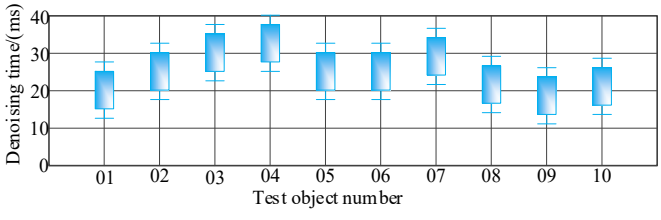

(b)

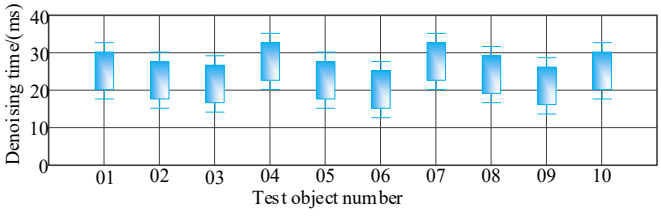

(c)

It can be seen from the analysis of Figure 5 that the proposed method can effectively reduce the denoising time of low-voltage current transformer defect image while effectively removing the noise of low-voltage current transformer defect image. The other two methods obtain significantly higher denoising of low-voltage current transformer defect image, which further verifies the advantages of the proposed method.

In order to further verify the advantages of the proposed method, different methods are used to detect and process the defects of low-voltage current transformers under the charged state. The detailed experimental test results are shown in Figure 6.

It can be seen from the analysis of Figure 6 that different methods are used to detect and process the defects of low-voltage current transformers under the charged state. The proposed methods can accurately detect various defects, while the other three methods cannot accurately detect relatively small defects in the detection process. It can be seen that the defect detection of low-voltage current transformer can be realised more accurately by using the proposed method.

Figure 6 Comparison of defect detection results of low-voltage current transformer under electrification by different methods, (a) proposed method (b) method of Hu et al. (2021) (c) method of Luo and Xu (2021) (d) method of Wang et al. (2021a) (see online version for colours)

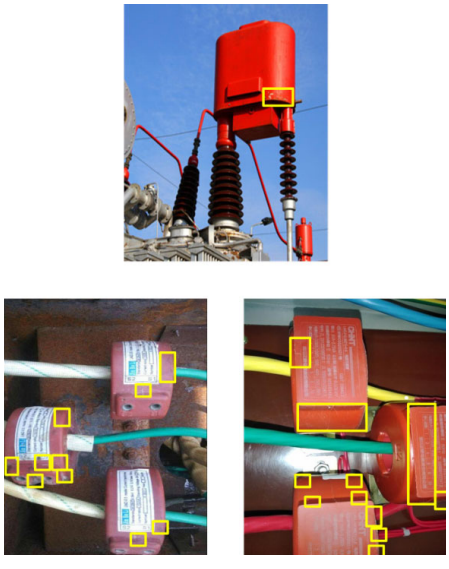

(a)

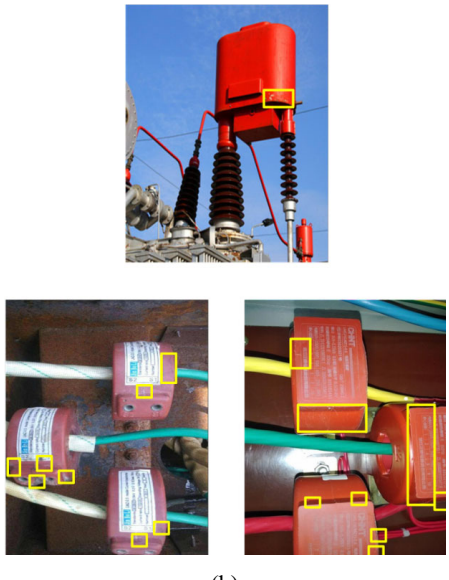

(b)

Figure 6 Comparison of defect detection results of low-voltage current transformer under electrification by different methods, (a) proposed method (b) method of Hu et al. (2021) (c) method of Luo and Xu (2021) (d) method of Wang et al. (2021a) (continued) (see online version for colours)

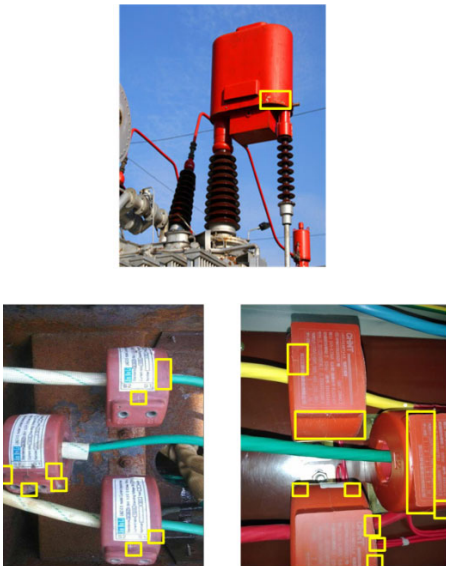

(c)

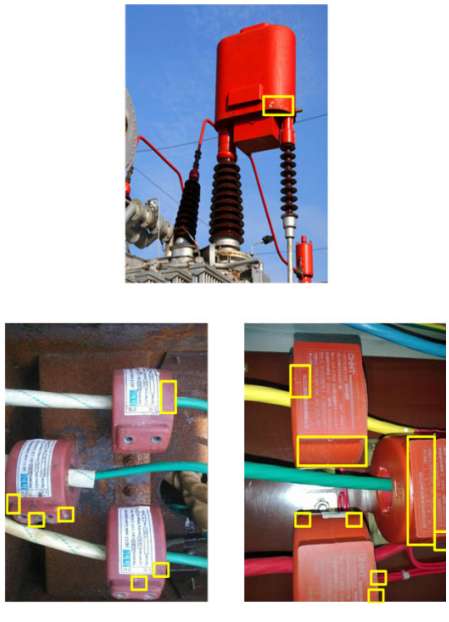

(d)

In order to further verify the detection performance of the proposed method, different types of low-voltage current transformer defects were detected and processed, and the leakage rate and false detection rate were used as test indicators. The detailed experimental results are shown in Tables 3 and 4.

Table 3 Comparison of experimental results of defect missing rate of low-voltage current transformers by different methods

Types of defects in low-voltage current transformers	*Missing detection rate (%)*			
	Proposed method	*Method of Hu et al. (2021)*	*Method of Luo and Xu (2021)*	*Method of Wang et al. (2021a)*
Corrosion	0.22	0.25	0.32	0.36
Scratch	0.15	0.18	0.23	0.27
Rust	0.17	0.20	0.25	0.30
Flaw	0.25	0.33	0.37	0.41
Worn	0.10	0.14	0.17	0.21
Stain	0.11	0.16	0.20	0.25
Fatigue wear	0.22	0.25	0.32	0.36

Table 4 Comparison of test results of defect false detection rate of low-voltage current transformers by different methods

Types of defects in low-voltage current transformers	*Inspection rate (%)*			
	Proposed method	*Method of Hu et al. (2021)*	*Method of Luo and Xu (2021)*	*Method of Wang et al. (2021a)*
Corrosion	0.35	0.40	0.44	0.48
Scratch	0.22	0.27	0.32	0.37
Rust	0.20	0.24	0.27	0.32
Flaw	0.31	0.35	0.41	0.45
Worn	0.17	0.22	0.26	0.27
Stain	0.13	0.17	0.22	0.25
Fatigue wear	0.30	0.35	0.39	0.44

It can be seen from the analysis of Tables 3 and 4 that after the defect detection and treatment of different types of low-voltage current transformers under the charged state, the values of the missing detection rate and the false detection rate obtained by the proposed method are significantly lower than those obtained by the other three methods, indicating that the proposed method can obtain accurate defect detection results of low-voltage current transformers.

In order to further verify the advantages of the proposed method, the following experimental tests mainly compare the change of defect detection time of low-voltage current transformers under different methods in the charged state. The detailed experimental test results are shown in Figure 7.

Figure 7 Comparison of test results of defect detection time of low-voltage current transformer with different methods under electrified state, (a) proposed method (b) method of Hu et al. (2021) (c) method of Luo and Xu (2021) (d) method of Wang et al. (2021a) (see online version for colours)

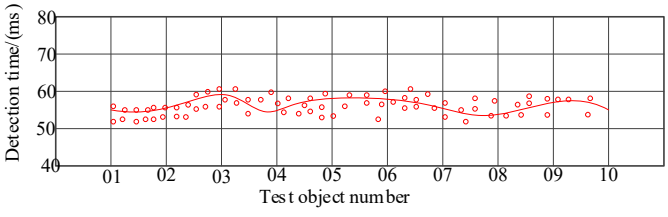

(a)

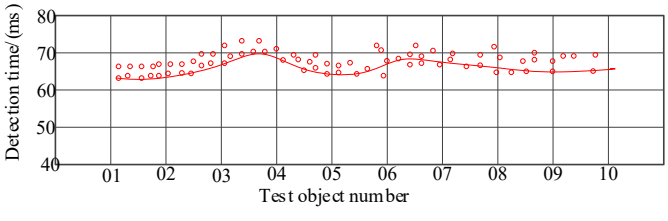

(b)

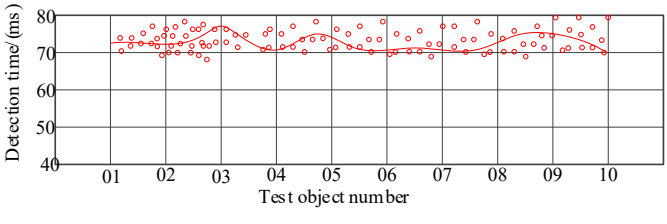

(c)

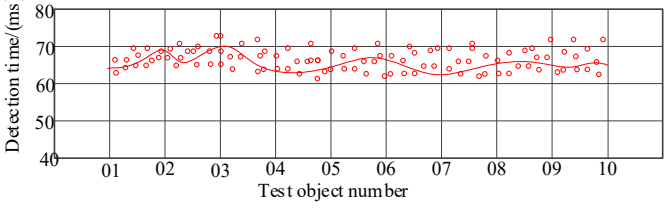

(d)

It can be seen from the analysis of Figure 7 that under different test samples, the defect detection time of low-voltage current transformer corresponding to each method has also changed significantly. Compared with the other three methods, the proposed method can complete defect detection of low-voltage current transformers at a faster speed, which can effectively improve the efficiency of defect detection of low-voltage current transformers, and further verify the advantages of the proposed method. This is because this method utilises the Hausdorff distance algorithm to efficiently extract the maximum difference between point sets, quickly obtain the position and shape information of defect areas, thereby reducing the time consumption for processing a large amount of data. The

calculation method of Hausdorff distance is simple and efficient, and does not require complex iteration or optimisation processes, therefore it has a relatively short computational time cost. In addition, to further improve detection efficiency, this method may adopt optimisation measures such as data preprocessing and parallel computing to reduce processing time.

4 Conclusions

In order to improve the operation reliability of low-voltage current transformer, a defect detection method of low-voltage current transformer based on Hausdorff distance algorithm under live state is proposed. The defect image of low-voltage current transformer under live state with noise is denoised, mainly by combining the bilateral filtering method and the joint probability distribution function. After taking the defect characteristics of low-voltage current transformer under electrification state, the Hausdorff distance algorithm and elastic diagram matching are effectively combined to complete the defect detection of low-voltage current transformer. The experimental results show that the proposed method can effectively improve the signal-to-noise ratio, reduce the Root-mean-square deviation, and obtain more satisfactory denoising results of the defect image of low-voltage current transformer in the charged state. Moreover, it can effectively improve the failure rate and false detection rate of defects of low-voltage current transformers under electrification, and obtain more accurate defect detection results of low-voltage current transformers under electrification.

Acknowledgements

Fund Project: 'Study on Live Working Inspection Technology to Test Metering Performance of Low-voltage Current Transformer' (520633220007), a Science and Technology Project of State Grid Shandong Electric Power Company.

References

Fan, J., Yang, C. and Udell, M. (2021) 'Robust non-linear matrix factorization for dictionary learning, denoising, and clustering', *IEEE Transactions on Signal Processing*, Vol. 69, No. 13, pp.1755–1770.

Guo, L.Y., Duan, H.Y., Zhou, W.W., Tong, G.H., Wu, J.H., Ou, X.F. and Li, W.J. (2022) 'Surface defect detection algorithm of magnetic tile based on mask R-CNN', *Computer Integrated Manufacturing Systems*, Vol. 28, No. 5, pp.1393–1400.

Guo, Y., Davy, A., Facciolo, G., Morel, J.M. and Jin, Q. (2021) 'Fast, nonlocal and neural: a lightweight high quality solution to image denoising', *IEEE Signal Processing Letters*, Vol. 23, No. 9, pp.149–156.

Hasan, F., Kargarian, A. and Mohammadi, J. (2021) 'Hybrid learning aided inactive constraints filtering algorithm to enhance AC OPF solution time', *IEEE Transactions on Industry Applications*, Vol. 57, No. 2, pp.1325–1334.

Hu, G.H., Wang, N., He, W.L. and Tang, H.X. (2021) 'Unsupervised surface defect detection method based on image in painting', *Journal of South China University of Technology (Natural Science Edition)*, Vol. 49, No. 7, pp.76–85, 124.

Hwang, S.W., Lee, T., Kim, H., Kim, H., Chung, H., Choi, J.G. and Yeo, H. (2022) 'Classification of wood knots using artificial neural networks with texture and local feature-based image descriptors', *Holzforschung*, Vol. 76, No. 1, pp.1–13.

Kong, L., Zhu, J. and Ying, S. (2021) 'Local stereo matching using adaptive cross-region-based guided image filtering with orthogonal weights', *Mathematical Problems in Engineering*, Vol. 56, No. 2, pp.1–20.

Luo, H. and Xu, G.L. (2021) 'Rail surface defect detection based on image enhancement and deep learning', *Journal of Railway Science and Engineering*, Vol. 18, No. 3, pp.623–629.

Qu, S., Qin, Z., Xu, Y., Cong, Z. and Liu, Z. (2021) 'High spatial resolution investigation of OFDR based on image denoising methods', *IEEE Sensors Journal*, Vol. 21, No. 17, pp.18871–18876.

Riya, H., Gupta, B. and Lamba, S.S. (2021) 'An efficient anisotropic diffusion model for image denoising with edge preservation', *Computers & Mathematics with Applications*, Vol. 93, No. 4, pp.106–119.

Wan, Y., Ma, A., He, W. and Zhong, Y. (2021) 'Accurate multi-objective low-rank and sparse model for hyperspectral image denoising method', *IEEE Transactions on Evolutionary Computation*, Vol. 41, No. 22, pp.367–375.

Wang, X., Kang, S. and Zhu, W.D. (2021a) 'Surface defect detection of AFP layers based on improved CenterNet', *Infrared and Laser Engineering*, Vol. 50, No. 10, pp.210–220

Wang, Y., Chang, D. and Zhao, Y. (2021b) 'A new blind image denoising method based on asymmetric generative adversarial network', *IET Image Processing*, Vol. 15, No. 6, pp.1260–1272.

Wei, Z. and Zhang, X. (2021) 'Feature extraction and retrieval of ecommerce product images based on image processing', *Traitement du Signal*, Vol. 38, No. 1, pp.181–190.

Yang, H., Gong, C., Huang, K., Song, K. and Yin, Z. (2021a) 'Weighted feature histogram of multi-scale local patch using multi-bit binary descriptor for face recognition', *IEEE Transactions on Image Processing*, Vol. 45, No. 11, pp.61–69.

Yang, J., Zhao, Y., Yang, S., Kang, X. and Cao, X. (2021b) 'Analysis of feature extraction and anti-interference of face image under deep reconstruction network algorithm', *Complexity*, Vol. 36, No. 2, pp.1–15.

Yao, Y., Wu, J., Lau, C., Wu, H. and Jiang, F. (2021) 'Reflection prediction of black silicon texture under the guidance of image recognition technology', *IEEE Journal of Photovoltaics*, Vol. 11, No. 3, pp.600–605.

Yu, H.T., Li, J.S., Liu, Y.J., Li, F.L., Wang, J., Zhang, C.H. and Yu, L.F. (2023) 'Section steel surface defect detection algorithm based on cascade neural network', *Journal of Computer Applications*, Vol. 43, No. 1, pp.232–241.